IJARSCT
ISSN (Online) 2581-9429
International Journal of Advanced Research in Science, Communication and Technology (IJARSCT)
International Open-Access, Double-Blind, Peer-Reviewed, Refereed, Multidisciplinary Online Journal
Impact Factor: 7.301
Volume 3, Issue 5, April 2023

A New Signal Processing Method Based on Notch Filtering and Wavelet Denoising in Wire Rope Inspection

Shubham Kamble[1], Badal Waghmare[2], Shivani Masram[3], Juhi Lad[4], Prof. Sagar Tarekar[5]
Student, Master of Computer Application[1,2,3,4]
Guide, Master of Computer Application[5]
Tulsiramji Gaikwad Patil College of Engineering and Technology, Nagpur, Maharashtra, India

Abstract: *Wire rope is a necessary tool in practical applications especially in crane, elevator and bridge construction, which plays an important role in the national economy and daily life, and safety inspection for wire rope is the key to ensure people's life and property. However, detection signals are usually complicated due to the twining structures, which make the wire rope defect signal and strand signal mix together. What's more, no reports and studies have appeared to solve this problem. In view of the situation and challenges above, this paper proposes a combined signal processing method based on notch filtering and wavelet denoising to process detected wire rope signals. Basic time domain, frequency domain and joint time–frequency analysis are first conducted, thereafter, conventional signal processing methods such as low-pass filtering and adaptive analysis are presented according to the signal characterizations. These comparisons and results demonstrate that a conventional single method is incapable of wire-rope-detection signal identification and differentiation. Nonetheless, after the notch filter design and calculation, the processing results for the typical wire rope inspection signals in the experiments indicate that the combined methods can not only distinguish steel wire rope defect signal and strand signal effectively but also with high detection accuracy, even for the inner defect. Finally, the feasibility and reliability are verified by a series of signal processing results and comparisons, which demonstrate that this new method has great application potential and is of vital significance to the development of wire rope safety inspection.*

Keywords: Wire rope - Signal processing - Notch filter - Wavelet denoising - Strand signal - Defect signal

I. INTRODUCTION

Wire rope plays a significant role in hoisting and loading in various industries. However, wire rope damage frequently occurs and the main forms are loss of metallic cross-sectional area (LMA) defect and local flaw (LF). Accordingly, the LMA sensor usually detects elongated metal losses such as produced by corrosion or wear, the LF sensor detects wire breaks. Furthermore, many studies have been conducted concerning the detection sensors for both LMA and LF defects, such as the giant magneto-resistive (GMR) sensor in, tunnel magneto-resistive (TMR) sensor in and coil or Hall-effect sensor in. Every sensor has a unique feature in wire rope detection, the key is to select. The application and detection scenarios. Primarily, coil sensors connected in series could be employed and perform well when sensing leakage fields in the radial, axial and tangential directions. A flexible GMR sensor array should be considered when detecting service-induced defects on the outer surface of steel track rope, but TMR devices as mentioned in may have superior performance in sensitivity and linear operation range over conventional magneto-resistive devices. Except for the inspection sensors, one of the biggest challenges and difficulties in wire rope defect detection is that the components of inspected signals are quite complex, thus, the methodology and technique of signal processing are the key in non-destructive testing (NDT) for steel wire ropes. In the last decades, the basic signal processing methods for steel wire rope mainly include time domain and frequency domain analysis as well as joint time–frequency analysis (JTFA). Among the techniques of time domain analysis; pre-amplifier, low pass filter, signal averaging, correlation analysis and adaptive methods are frequently applied. On the other hand, wire rope signal processing methods in frequency domain generally refer to the traditional fourier transform, fast fourier transform (FFT), amplitude-frequency and phase-

IJARSCT
ISSN (Online) 2581-9429
International Journal of Advanced Research in Science, Communication and Technology (IJARSCT)
International Open-Access, Double-Blind, Peer-Reviewed, Refereed, Multidisciplinary Online Journal
Impact Factor: 7.301
Volume 3, Issue 5, April 2023

frequency characterization analysis. which all make the defect detection and signal differentiation more complicated. Hence, single signal processing methods seem to be in vain in defect detection and signal differentiation, another problem is the interference of noise such as background noise of geomagnetic field in the MFL testing and the noise produced by relative movement between detection devices and wire ropes, therefore, signal denoising is also of great significance, the technique of wavelet denoising appeared, it has developed rapidly and overcome the disadvantages of invariability of time–frequency window in Fourier transform, thereafter, becoming an ideal tool for time and frequency domain signal analysis. The most remarkable characterization of wavelet analysis is that it can be applied to local analysis in time and frequency domain by its flexible scale and time shift operation as well as the abundant functions. Finally, it can refine high-frequency signals in time domain and low-frequency signals in frequency domain and therefore

II. EXPERIMENTAL APPARATUS AND SPECIMENS

To obtain original detection signals from wire rope specimens, large number of experiments were conducted. The experimental apparatus and specimen details are introduced in this section. As NDT theories and techniques develop rapidly, they have become the prevalent and dominant methods in steel wire rope inspection. Among these NDT techniques in steel wire ropes detection, MFL testing is one of the most frequently and effectively used methods. The basic MFL testing principles for steel wire rope defect detection are briefly illustrated in Fig. 1. Two sets of permanent magnets, located above the wire rope surface and joined by magnet yoke, are used to magnetize the specimen of the tested wire rope, then, the magnetic circuit will be formed in the permanent magnet, magnetic yoke, air gap and wire rope. When the defects (inner defects or outer types) have occurred, part of the magnetic flux leaks out due to the sudden change to low permeability and high magnetic resistance. After that, the detecting device composed of magnet yoke, permanent magnet and sensors scans along the axis direction of the wire rope.

As mentioned above, the practical experimental apparatus is shown in Fig. 2. The detecting apparatus is mainly composed of permanent magnet, magnetic yoke and internal Hall-effect sensors. Actually, the sensor used here could be viewed as a point detector, which measures the field in a very small area. These sensors are evenly distributed around the circumference of the rope and embedded inside the detecting apparatus, thus the strand signals could be averaged and a good broken wire signal-to-noise ratio is produced. After the tested wire ropes are magnetized and scanned repeatedly by the detecting apparatus, the corresponding inspection signals from Hall-effect sensors are captured and acquired.

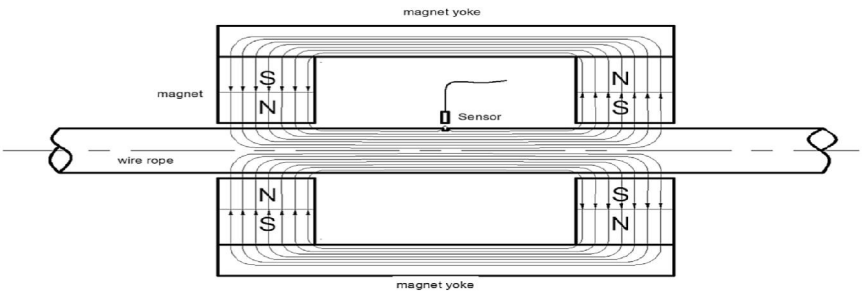

Fig. 1 Brief principles of MFL testing for wire rope

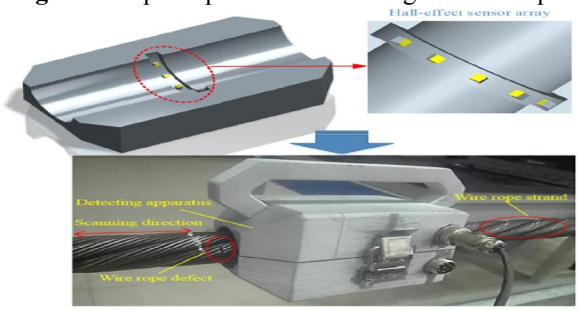

Fig. 2 Practical experimental apparatus for wire rope

IJARSCT
ISSN (Online) 2581-9429
International Journal of Advanced Research in Science, Communication and Technology (IJARSCT)
International Open-Access, Double-Blind, Peer-Reviewed, Refereed, Multidisciplinary Online Journal
Impact Factor: 7.301
Volume 3, Issue 5, April 2023

In practical applications, wire ropes often suffer from various forms of damage, which include LF defect and LMA defects as a result of working conditions. The forms of damage can be generally divided into deformation, fatigue failure, abrasion, corrosion and wire breakage by different causes. To be more explicit, LF defects are mainly analysed here and these defects could be classified into outer defects and inner types by the damage locations on wire ropes and difficulty in detection. Naturally, there are three typical defects, namely, Naturally, to verify the validity and reliability of the proposed combined methods, three typical defect signals are acquired by a series of experiments and the corresponding practical specimens are expressed in Fig. 3a–c.

As shown in Fig. 3, outer multiple broken wires mean that multiple wires break simultaneously in a strand and the defect is located on the surface of the wire rope. Similarly, inner broken wire defect means that these defects hide inside the strands or groove and locate farther from the surface compared with outer defects. Additionally, the tested wire ropes consist of six strands, which twine together helically in structures, and the largest outer diameter is 30 mm, the single diameter of a strand which is composed of 10 twining wires is approximate to 8 mm, and the minimum wire diameter is 1.4 mm.

III. CONVENTIONAL METHODS OF WIRE ROPE

3.1 Signal Processing

To verify the reliability and feasibility of the above mentioned combined method based on notch filtering and wavelet denoising, comparisons with these conventional signal processing methods were conducted. Basic features of the typical wire rope strands and defect signals were first analysed, namely, time domain analysis, fast Fourier transform (FFT) analysis and joint time–frequency analysis (JTFA).

Typical wire rope strand and defect signals in time domain acquired by experimental apparatus and related data acquisition modules in Fig. 2 are shown in Fig. 4, where wire rope strand signal and typical detection signal containing

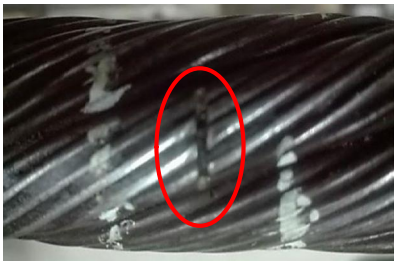

(a) Specimen of outer multiple broken wires defect in the experiments

(b) Specimen of outer single broken wire defect in the experiments

(c) Specimen of inner single broken wire defect in the experiments

Fig. 3 Specimens with typical wire rope defects

IJARSCT
ISSN (Online) 2581-9429
International Journal of Advanced Research in Science, Communication and Technology (IJARSCT)
International Open-Access, Double-Blind, Peer-Reviewed, Refereed, Multidisciplinary Online Journal
Impact Factor: 7.301
Volume 3, Issue 5, April 2023

Defects are expressed in Fig. 4a and b, respectively. Particularly, the horizontal axis of 'sampling count' means the amount of signal sampling point, which is positively waveform, but the defect signals mixed with noise stand out in amplitude and are surrounded by homogeneous strand signals. These features are especially remarkable when the defect is relatively large in size and adjacent to the surface. However, wire rope defects not only appear in the surface, but also hide inside of the wire rope structures in practice, which increases the detection difficulty vastly. Except for the preliminary analysis in time domain, a calculation by FFT and short time fourier transform (STFT) for the typical wire rope strand and defect signals was further conducted, and the amplitude spectrum of typical strand and defect signals in Fig. 4 is illustrated in Fig. 5, respectively. The signal characterization in frequency domain is that both strand and defect signal frequencies are very low and distributed in an extremely narrow range from 0 to 10 Hz, the possible reason for this phenomenon is that the data acquisition system is connected with an anti-aliasing lowpass filter. Other influence factors may be the scanning speed of the sensor and the structure of the wire rope as well as the distance between two continuous defects. Meanwhile, the frequency distribution regularities are almost the same,related to sampling time but has no unit. Observed by these representative signals, a preliminary characterization indicated that the signal amplitude of wire rope strand is evenly distributed and resembles high-frequency sinusoidal.

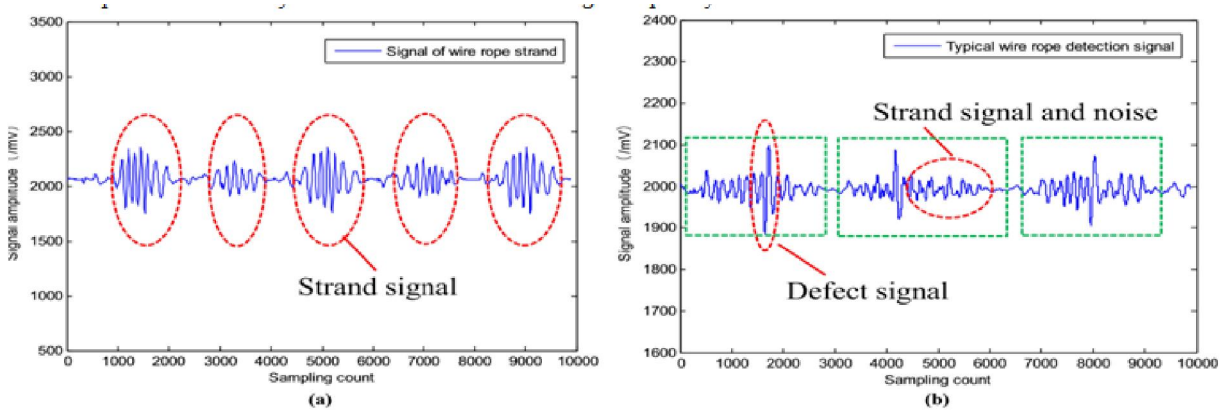

Fig. 4 Typical wire rope strand and defect signals in time domain

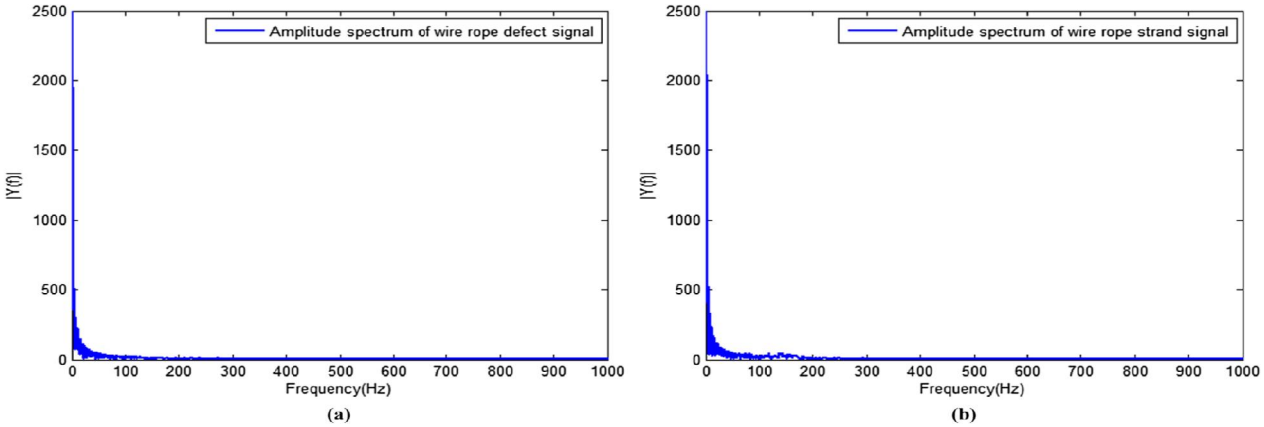

Fig. 5 FFT of typical wire rope strand and defect signals in Fig. 4

Which makes the two types of signal differentiation, from the perspective of single frequency analysis, almost impossible. In addition, signals in other frequency ranges are weak and could be omitted after signal pre-processing through hardware electric circuit.

Similarly, Fig. 6 shows the spectrum of JTFA after STFT processing for the typical signals in Fig. 4, from which we can also conclude that the acquired signal frequencies distribute in 0 to 150 Hz and the features in frequency domain is consistent with that shown in Fig. 5. To be more specific, Fig. 6a represents the STFT spectrum of wire rope strand signals and the five spectrum fragments exactly coincide with the five strand signals acquired by scanning five times and shown in Fig. 4a, judging by the spectrum colour, it can be observed that the lower the frequency is, the stronger the amplitude is in the spectrum fragments.

IJARSCT
ISSN (Online) 2581-9429
International Journal of Advanced Research in Science, Communication and Technology (IJARSCT)
International Open-Access, Double-Blind, Peer-Reviewed, Refereed, Multidisciplinary Online Journal
Impact Factor: 7.301
Volume 3, Issue 5, April 2023

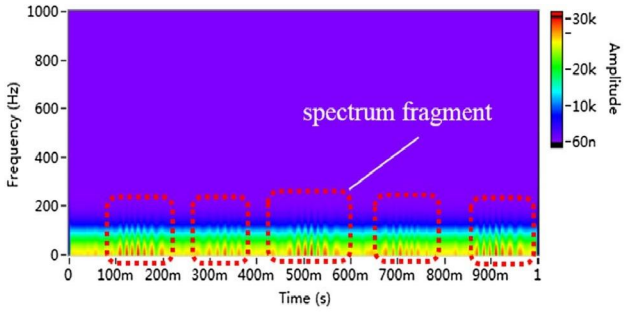

(a) STFT spectrum of wire rope strand signal

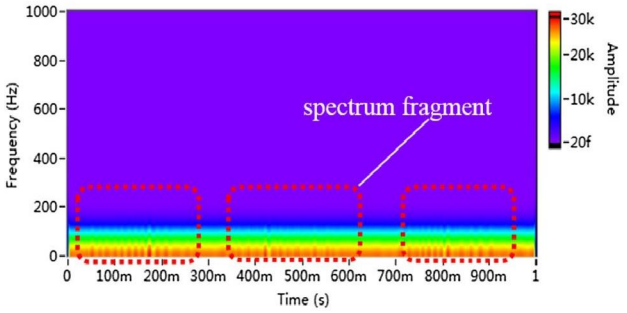

Fig. 6 Joint time–frequency analysis by STFT aSTFT spectrum of wire rope strand signal. **b** STFT spectrum of typical wire rope defect signal

To demonstrate the validity and feasibility of the proposed combined method further, a comparison between conventional wire rope signal processing method and the new one is conducted. The conventional wire rope signals processing method of low pass filtering is applied first, as shown in Fig. 7. To be more precise, a two order Butterworth lowpass filter is selected, and when the lowpass cut-off frequency is chosen as 150 Hz, 100 Hz, 80 Hz, 50 Hz and 20 Hz, lowpass filtering results of typical wire rope strand and defect signals in Fig. 4 are illustrated in Fig. 7a–e, respectively.

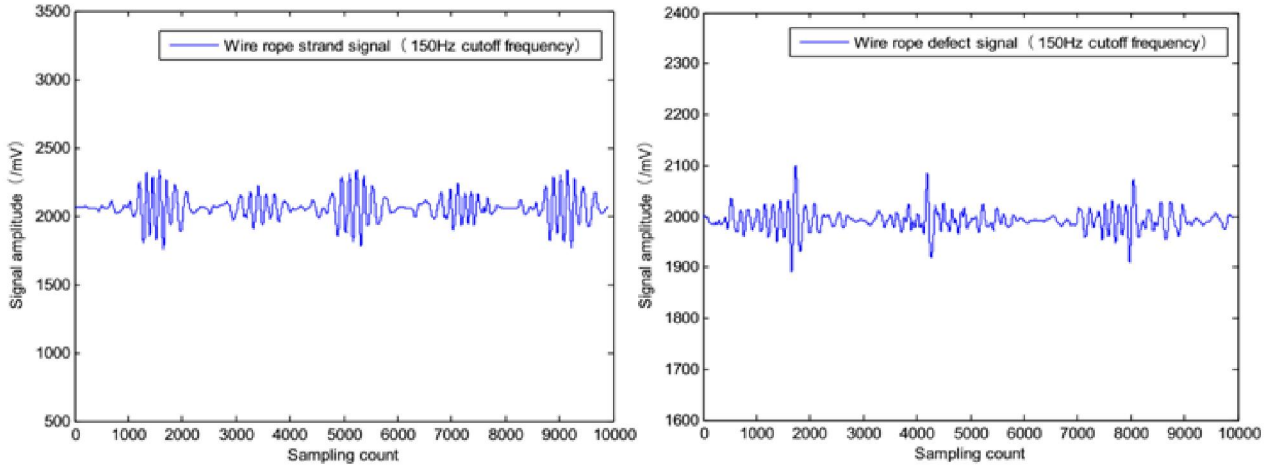

(a) 150Hz cutoff frequency of lowpass filtering

IJARSCT
ISSN (Online) 2581-9429
International Journal of Advanced Research in Science, Communication and Technology (IJARSCT)
International Open-Access, Double-Blind, Peer-Reviewed, Refereed, Multidisciplinary Online Journal
Impact Factor: 7.301
Volume 3, Issue 5, April 2023

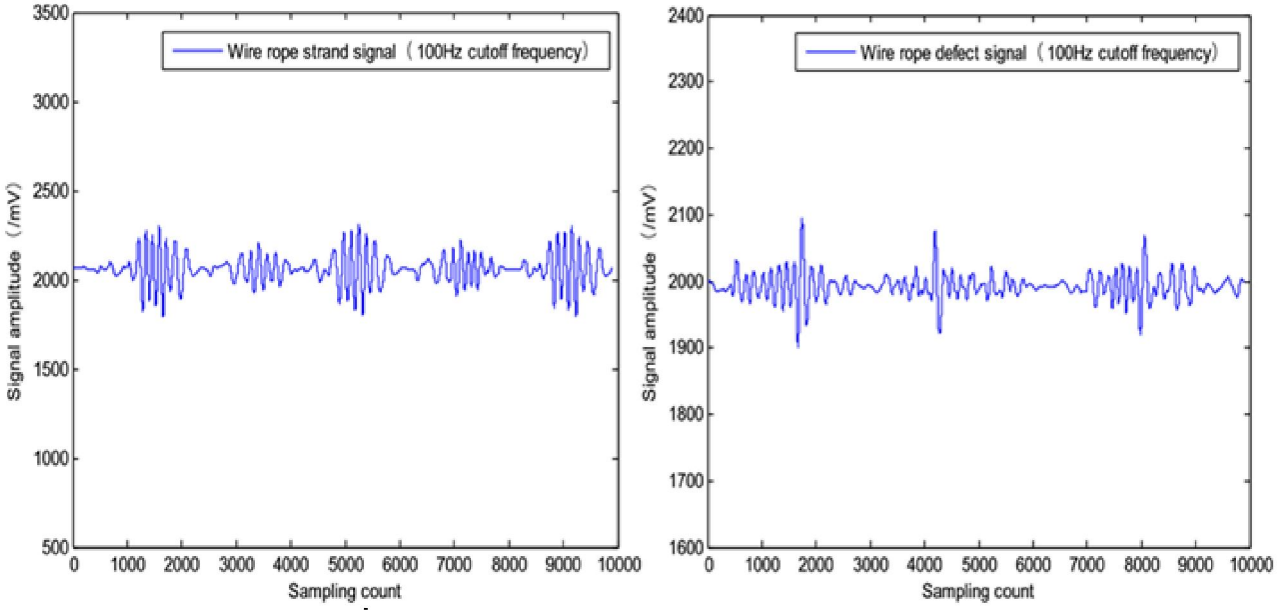

(b) 100Hz cutoff frequency of lowpass filtering

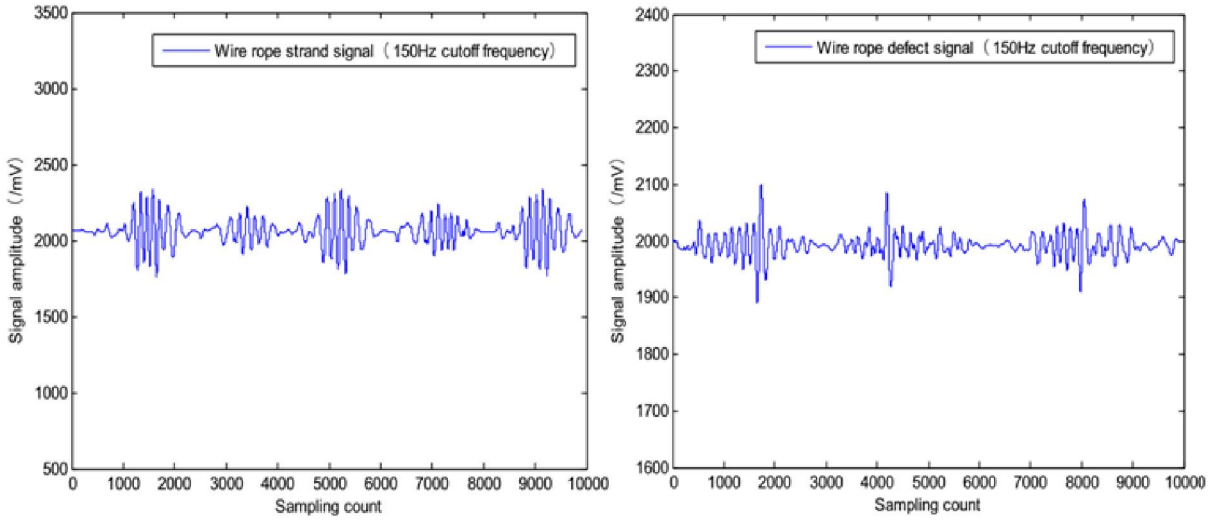

(c) 80Hz cutoff frequency of lowpass filtering

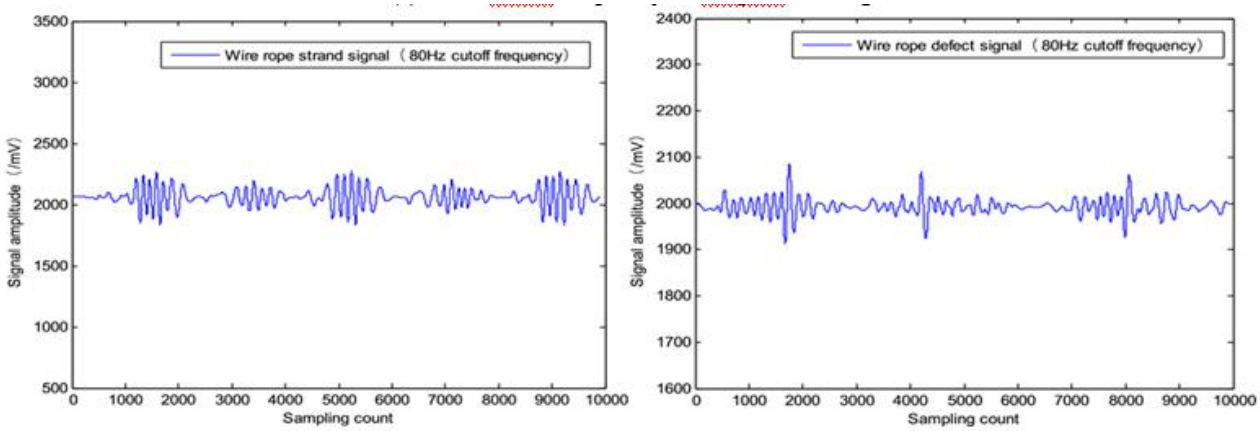

Fig. 7 Wire rope detection signals processed by lowpass filter. a tiring d 50 Hz cutoff frequency of lowpass filtering. e 20 Hz cutoff

IJARSCT
ISSN (Online) 2581-9429
International Journal of Advanced Research in Science, Communication and Technology (IJARSCT)
International Open-Access, Double-Blind, Peer-Reviewed, Refereed, Multidisciplinary Online Journal
Impact Factor: 7.301
Volume 3, Issue 5, April 2023

(d)150 Hz cutoff frequency of lowpass filtering. b 100 Hz cutoff pre- frequency of lowpass filtering quency of lowpass filtering. c 80 Hz cutoff frequency of lowpass fil-

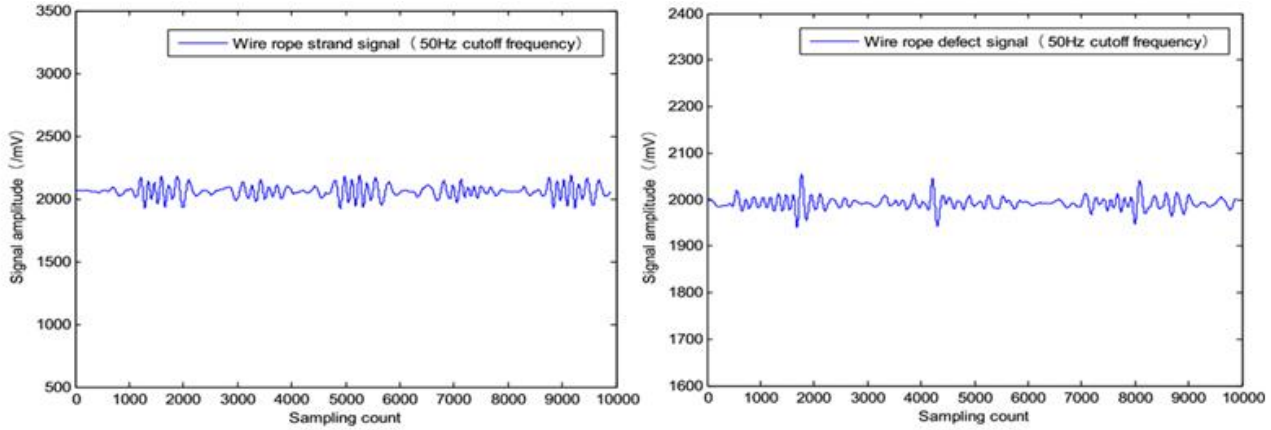

(d) 50Hz cutoff frequency of lowpass filtering

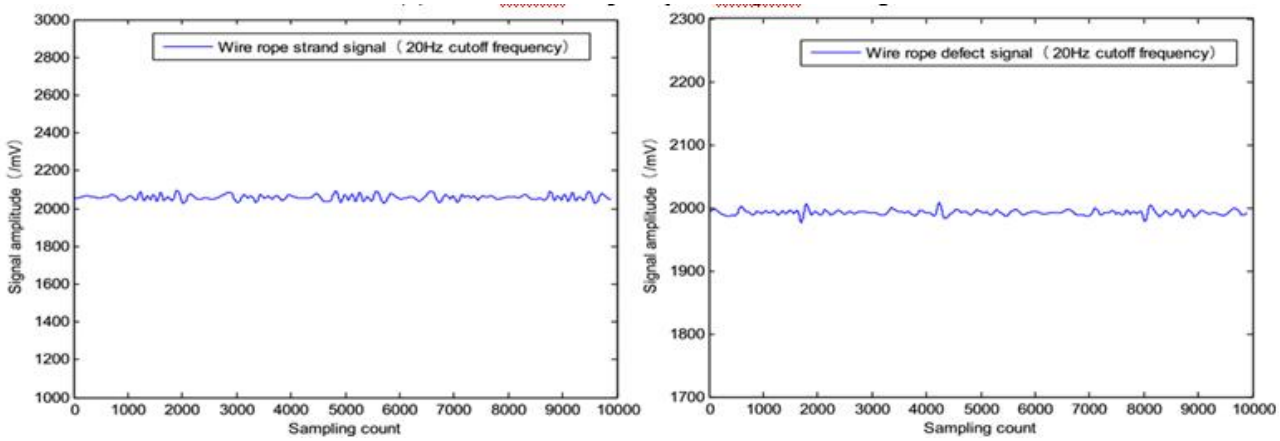

(e) 20Hz cutoff frequency of lowpass filtering

Drawn that when the cutoff frequency is larger than 50 Hz, lowpass filtering is almost ineffective at eliminating strand signal and noise, while it's valid and effective when the cutoff frequency is less than 50 Hz, which further indicates that the strand signal frequency occurs under 50 Hz. Finally, Fig. 7e shows that although the strand signals are eliminated in some extentAccording to the wire rope strand and defect signal characterization in time domain, a basic feature in signal amplitude is that the wire rope strand signal is evenly distributed, while the defect signal always contains a relative outstanding peak in waveform. Therefore, another signal processing method based on wavelet hard threshold denoising is investigated to differentiate these two typical signals. The denoising results of this method is described as follows, where, x is the time series signal, T is the threshold value of $\cdot|\ |\ \phi(x) = x\ 1\ \{x > T\}(1)$ wavelet hard threshold denoising. When the signal amplitude is bigger than the set threshold value of T, the signal will remain unchanged as x; conversely, when the signal amplitude is smaller than T, the time series signal will be 0. By setting different threshold value of T, signal processing results are presented in Fig. 8.

IJARSCT
ISSN (Online) 2581-9429
International Journal of Advanced Research in Science, Communication and Technology (IJARSCT)
International Open-Access, Double-Blind, Peer-Reviewed, Refereed, Multidisciplinary Online Journal
Impact Factor: 7.301
Volume 3, Issue 5, April 2023

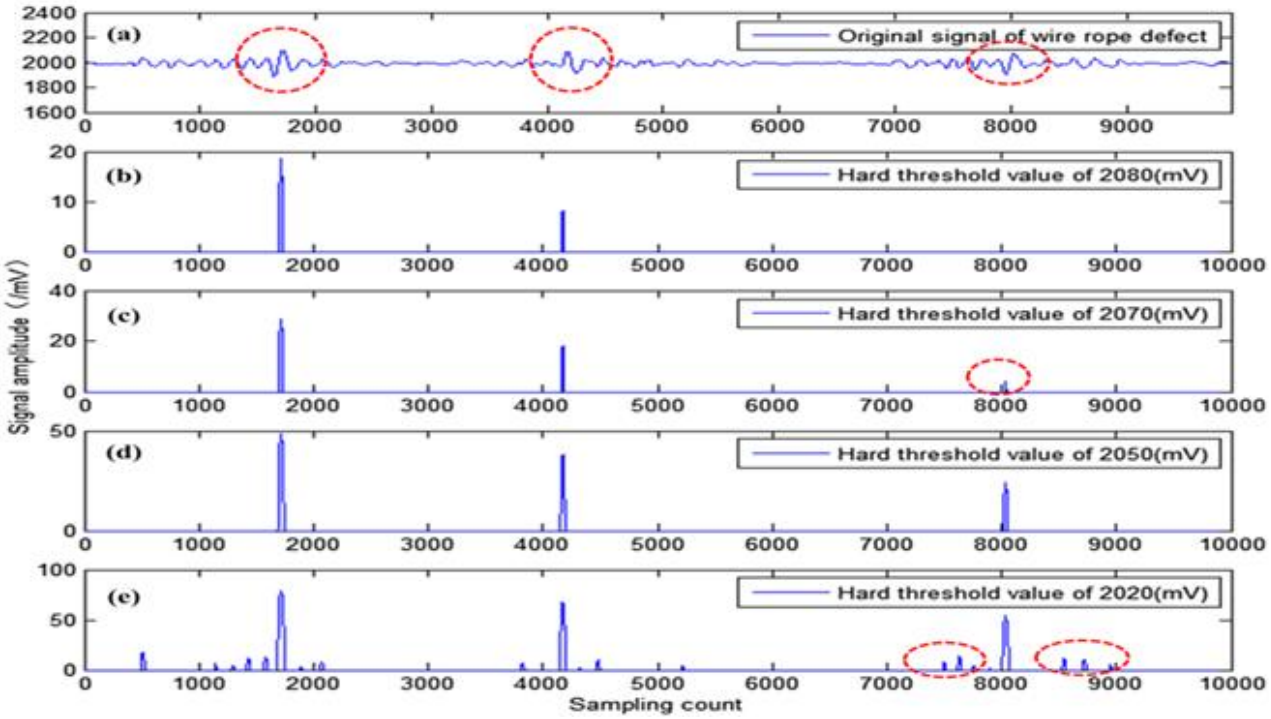

Fig. 8 Hard threshold wavelet denoising for wire rope defect signals

be more specific, when the threshold value is 2080 mV, only two defects were identified, which can be observed by the two peaks in the waveform in Fig. 8b, apparently, this may lead to the missing detection. Although there exists three defect signal waveforms in Fig. 8cd for quantitative evaluation of wire rope defect size. The evident signal waveform in Fig. 8d shows that the hard threshold value of 2050 mV is suitable for wire rope defect identification and detection, because not any strand signal or noise is present. As a consequence, the adaptive analysis method is taken into consideration. According to the related literature. Signal series of x[i] can be defined as follows,

$$x[i] = \sum_{k=0}^{N-1} A_k h_k[i] \quad (2)$$

where the signal of x[i] can be decomposed as a sum of weighted linear adaptive modulated Gaussian function, Ak is the weight of each individual hk[i], N denotes the total number of elementary functions used by hk[i], and the adaptive Gaussian function of hk[i] is defined by the following,

$$h_k[i] = (\alpha_k \pi) \exp\{-0.25\,[i - i_k]^2\}\exp\{-2\alpha_k + j\,2\pi f_k[i - i_k]\} \quad (3)$$

Where the function of hk[i] has three parameters: αk, ik and fk. The accuracy of the adaptive analysis will increase along with the number of decomposed elementary function; When the decomposed number of N is 41, the strand signals are relatively smaller and the degree of distortion of defect signal is the least. However, an appropriate decomposed number of N should be selected first through this method, which increases the difficulty and decreases the efficiency for wire rope defect detection in practical applications.

IV. NOTCH FILTERING AND WAVELET DENOISING METHODS

4.1 Theoretical Background of the Combined Methods

According to the signal processing and analysis results including time domain, frequency domain and JTFA for wire rope strand inspection and defect detection mentioned above, we can confirm that the conventional single signal processing methods, such as butterworth lowpass filtering, wavelet hard threshold denoising and adaptive analysis fail to complete the task of wire rope strand and defect signal identification and differentiation, consequently, a new combined signal processing method based on notch filtering and wavelet denoising is presented.

IJARSCT
ISSN (Online) 2581-9429
International Journal of Advanced Research in Science, Communication and Technology (IJARSCT)
International Open-Access, Double-Blind, Peer-Reviewed, Refereed, Multidisciplinary Online Journal
Impact Factor: 7.301
Volume 3, Issue 5, April 2023

(0) 2

α_p = 10lg|$_H H_{aj\omega j}$ p|||||$_2$dB (4)

|||a()Sampling count

Where, α_p is the maximum attenuation in the passband, $H_a(j\omega_p)$ is the amplitude-frequency characteristic. After normalization processing, namely, let $|H_a(j0)| = 1$, Eq. (4) can be calculated as,

$\alpha_p = -10\lg|H_a(j\omega_p)|^2$ (5)

By further calculation or transformation for Eqs. (5) and (6

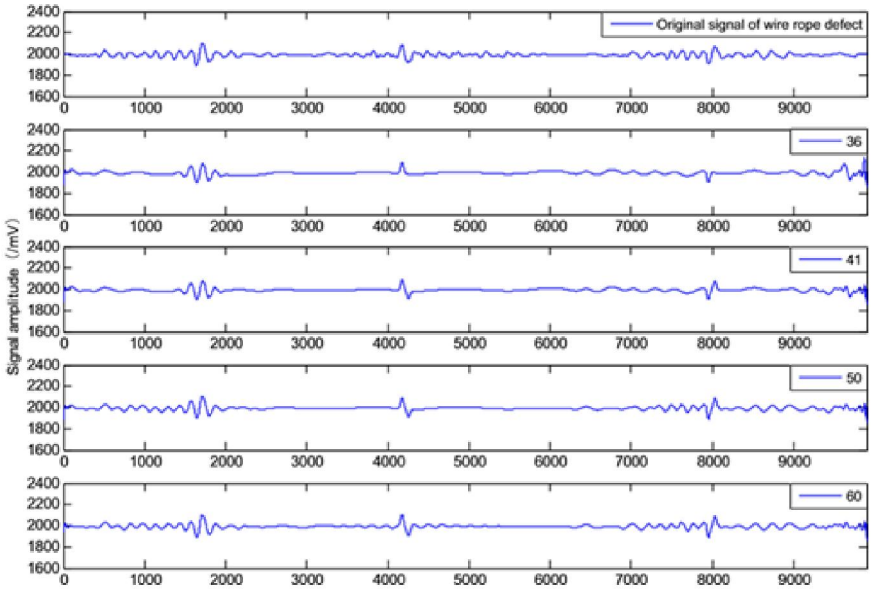

Fig. 9 Adaptive analysis of wire rope defect signals

design a notch filter referred to as a bandstop filter.

1 0.1α= 10 $_p$

2 (6) ||Ha($j\omega p$)|||

Since the square amplitude function of a Butterworth lowpass filter satisfies the following equation,

1

| $H_a(j\omega_p)|^2 = 1+(\omega p/\omega c)2N$ (7)

where, ω_p is the cutoff frequency in the passband, ω_c is the cutoff frequency in the attenuation of 3 dB, N is the order of the filter. Combining (6) with (7), the following relationship,

1 0.1α_p

1+($\omega p/\omega c$)2N = 10 (8) is obtained. By further calculation and transformation of (8),

($\omega p\omega c$)N = $\sqrt{100.1\alpha p - 1}$ (9) is obtained. Similarly, for the cutoff frequency of ω_s , is used to obtain the following equation,

($\omega_s\omega_c$)^N = $\sqrt{100.1^{\alpha_s} - 1}$ (10) where, α_s is the minimum attenuation in the stopband. When Eq. (10) is divided by (9) in both sides, Eq. (11) is obtained as,

$$(\omega_s/\omega_p)^N = \sqrt{\frac{10^{0.1\alpha_s} - 1}{10^{0.1\alpha_p} - 1}} \quad (11)$$

Since the normalized passband frequency of lowpass filter satisfies ω_p = 1, the next step is to calculate the normalized stopband frequency of ω_s . On the other hand, the normalized lowpass frequency of ω and bandstop frequency of μ satisfy the following,

ω=μ2 −$\mu_0$2 (12) where, μ_0 is the normalized bandstop centre frequency, according to the relationship between the normalized lowpass frequency of ω and bandstop frequency of , the relations,

μ_s1

ω_{s1} = 2

IJARSCT
ISSN (Online) 2581-9429
International Journal of Advanced Research in Science, Communication and Technology (IJARSCT)
International Open-Access, Double-Blind, Peer-Reviewed, Refereed, Multidisciplinary Online Journal
Impact Factor: 7.301
Volume 3, Issue 5, April 2023

$$\begin{cases} \mu s21 - s2\mu 02^2 \\ -\omega s2 = s2 \\ \mu - \mu 0 \end{cases} \quad (13)$$

are obtained. According to the equation set of (13), the normalized stopband frequency of ω_s is given by,

$\omega_s = \min(\omega/s_1, |p\omega_{s2}|)$ (14)

If we let $\omega s / \lambda^N = k$, then Eq. (9) can be transformed as,

$$= \sqrt{\frac{10^{0.1\alpha s} - 1}{10^{0.1\alpha p} - 1}} = \quad (15)$$

If α_p and α_s are known beforehand, taking the logarithm of Eq. (15) on both sides, and thus the filter order can be calculated as,

$\lg k^{N=} \lg \lambda$ (16)

Since the normalized transfer function can be expressed as,

$H_a(p) = 1/B(p)$ (17) where, p is the normalized complex frequency and satisfies $p = j\omega/\omega_c$, $B(p)$ is a denominator polynomial and satisfies the following equation,

$B(p) = pN + bN-1pN-1 + bN-2pN-2 + \cdots + b1p + b0$ (18) where, b_0, b_1…, b_{N-1} are coefficients of denominator polynomials.

$H_{bs}(s) = H_a(p)|_{p=s} 2sB + \omega 2$ (20)

Based on the calculations above, the design for the notch filter is completed. However, when differentiating the wire rope strand and defect signals by notch filter, noise is unavoidable, especially in the detection process of sampling and scanning. Therefore, wavelet denoising is considered.

Since the conventional denoising methods including linear and nonlinear filtering methods such as median and Wiener filtering cannot describe the non-stationary characterization and correlation of signals, wavelet transformation possesses multiresolution features and is thereby, available to describe non-stationary characterization of signals. Thus, appropriate wavelet basis is capable of signal denoising in wire rope defect detection. To be more explicit, continuous wavelet transform (CWT) is applied for wavelet denoising, and the definition is as follows,

$$WT_x(a,\tau) = \frac{1}{\sqrt{a}} \int_{-\infty}^{\infty} s(t)\psi^*\left(\frac{t-\tau}{a}\right) dt \quad (21)$$

where, $s(t)$ is the wire rope sampling signals in time domain, $\Psi(t)$ is the mother wavelet function, τ is the time shift and a is the scale of wavelet transformation.

According to the characterization of wire rope detection signals after notch filtering, db6 basis function in the Daubechies series is selected as the mother wavelet function, and the wavelet decomposition level is 12. The concrete soft-threshold function (also called the shrinkage function) is, where, $\eta(x)$ is the denoising function, $\cdot\,||\,x$ is the time series.

4.2 Signal Processing Results

The most obvious outer multiple broken wires defect signals are processed and analysed first. After scanning and detecting for multiple broken wire defects shown in Fig. 3a by the experimental apparatus expressed in Fig. 2, the corresponding signals are obtained and illustrated in Fig. 10. The results shown in Fig. 10a–c are original wire rope detection signals, notch filter processed signal and wavelet denoising signal, respectively Although the defect signals are mixed with strand signals, by the former frequency domain analysis, it can be observed that most of the signal frequencies distribute in the range of 0–150 Hz, thus, the upper and lower cutoff frequency of the notch filter could be set as 200 Hz and 10 Hz, respectively, the passband attenuation is 0.5 dB, the maximum stopband attenuation is 20 dB and the sampling rate is 9900. According to the notch filter processed results in Fig. 10b, it can be observed that most of the strand signals around the defect signals are eliminated, which makes the defect signals become more obvious. After being processed by 12 levels of db6 wavelet soft threshold denoising in Fig. 10c

Similarly, after scanning and detecting for outer single broken wire defect shown in Fig. 3b by the MFL testing apparatus from Fig. 2, the corresponding signals are obtained and presented in Fig. 11a–c. The sectional area of outer

IJARSCT
ISSN (Online) 2581-9429
International Journal of Advanced Research in Science, Communication and Technology (IJARSCT)
International Open-Access, Double-Blind, Peer-Reviewed, Refereed, Multidisciplinary Online Journal
Impact Factor: 7.301
Volume 3, Issue 5, April 2023

single broken wire defect is less than that of the outer multiple broken wire, thereafter, the MFL strength is weaker which can be seen from the signal amplitude of original signal in Fig. 11a.

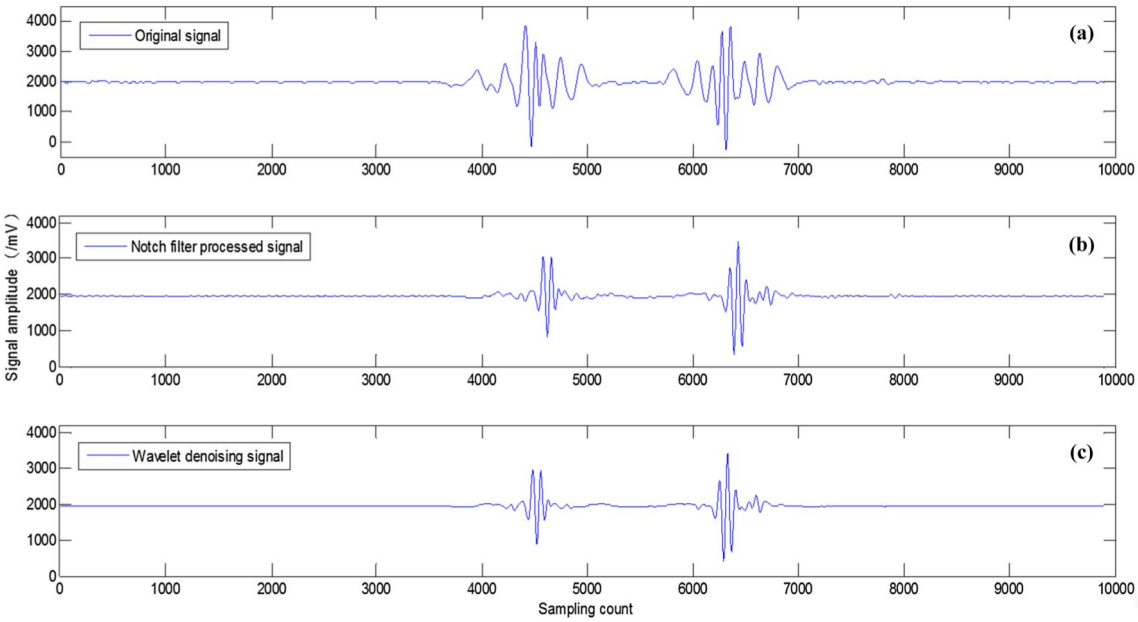

Fig. 10 Signal processing results of multiple wire rope broken defects

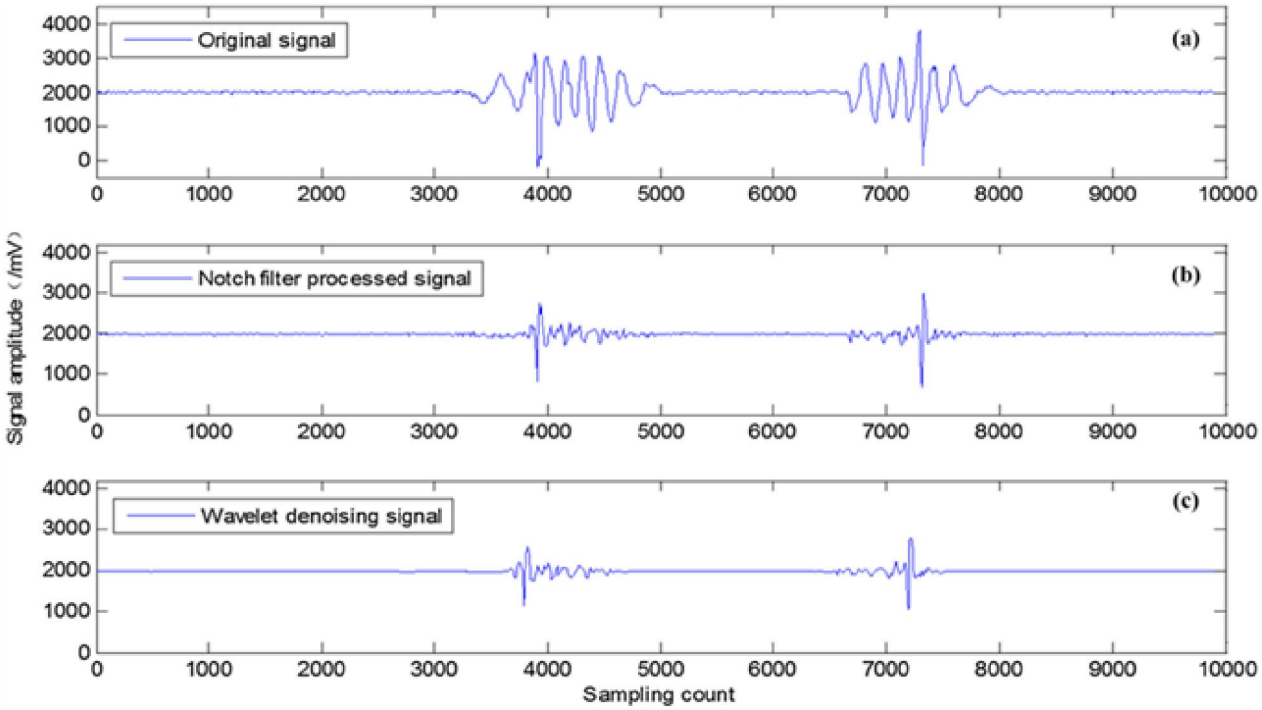

Fig. 11 Signal processing results for single outer broken wire defect of wire rope

IJARSCT
ISSN (Online) 2581-9429
International Journal of Advanced Research in Science, Communication and Technology (IJARSCT)
International Open-Access, Double-Blind, Peer-Reviewed, Refereed, Multidisciplinary Online Journal
Impact Factor: 7.301
Volume 3, Issue 5, April 2023

Fig. 12 Signal processing results for single inner broken defect and **Fig. 13** Signal processing results for wire rope strand without defect

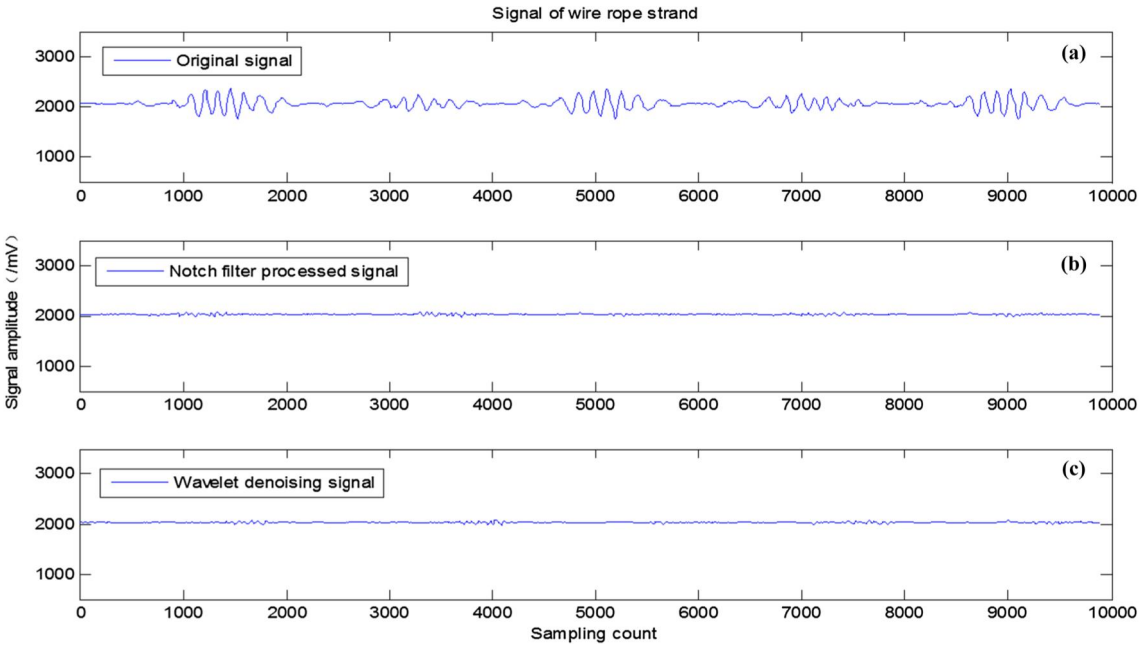

The experimental apparatus is the same with that mentioned above and expressed in Fig. 2, after scanning anddetecting for the wire rope strand, corresponding signals were obtained and are shown in Fig. 13. To keep consistent with the signal processing procedures above, original wire rope strand signal, notch filter processed signal and the final wavelet soft threshold denoising processed signal are separately shown in Fig upper and lower passband cutoff frequencies for the notch filter are 200 Hz and 10 Hz, and the 12 levels of db6 wavelet basis is selected for denoising. Finally, as presented in Fig. 13c, all the original strand signals are eliminated. Thus, the validity of this method is verified. All in all, among the series of experiments and results described above.

V. CONCLUSION

From the perspective of theoretical calculation, experimental verification and comparison with conventional wire rope signal processing techniques, a combined signal processing method based on notch filter and wavelet denoising is proposed. It turns out that this method is effective in wire rope defect and strands signal differentiation and improves the SNR to a great extent. Additionally, the feasibility and reliability are demonstrated through a series of experiments and processing results. Therefore, this new method has great application promise and plays an important role towards the development of wire rope safety inspection

The heading of the Acknowledgment section and the References section must not be numbered. Causal Productions wishes to acknowledge Michael Shell and other contributors for developing and maintaining the IEEE LaTeX style files which have been used in the preparation of this template.

REFERENCES

[1]. Kalwa, E., Piekarski, K.: Design of inductive sensors for magnetic testing of steel ropes. NDT Int. 20(6), 347–353 (1987)

[2]. Casey, N., White, H., Taylor, J.: Frequency analysis of the signals generated by the failure of constituent wires of wire rope. NDT Int. 18(6), 339–344 (1985)

[3]. Rizzo, P., di Scalea, F.L.: Ultrasonic inspection of multi-wire steel strands with the aid of the wavelet transform. Smart Mater. Struct. 14(4), 685 (2005)

IJARSCT
ISSN (Online) 2581-9429
International Journal of Advanced Research in Science, Communication and Technology (IJARSCT)
International Open-Access, Double-Blind, Peer-Reviewed, Refereed, Multidisciplinary Online Journal
Impact Factor: 7.301
Volume 3, Issue 5, April 2023

[4]. Kerschen, G., Lenaerts, V., Marchesiello, S., Fasana, A.: A frequency domain versus a time domain identification technique for nonlinear parameters applied to wire rope isolators. J. Dyn. Syst. Meas. Contr. 123(4), 645–650 (2001)

[5]. Rizzo, P., Di Scalea, F.L.: Wave propagation in multi-wire strands by wavelet-based laser ultrasound. Exp. Mech. 44(4), 407–415 (2004)

[6]. Song, E., Shin, Y.-J., Stone, P.E., Wang, J., Choe, T.-S., Yook, J.-G., Park, J.B.: Detection and location of multiple wiring faults via time–frequency-domain reflectometry. IEEE Trans. Electromagn. Compat. 51(1), 131–138 (2009)

[7]. Allen, R.L., Mills, D.: Signal Analysis: Time, Frequency, Scale, and Structure. Wiley, New Jersey (2004)

[8]. Jomdecha, C., Prateepasen, A., Methong, W.: Characterization of wire rope defects from magnetic flux leakage signals. Thammasat Int. J. Sci. Technol. 8(1), 54–63 (2003)

[9]. Welch, P.: The use of fast Fourier transform for the estimation of power spectra: a method based on time averaging over short, modified periodograms. IEEE Trans. Audio Electroacoust. 15(2), 70–73 (1967)

[10]. Bendat, J.S., Piersol, A.G.: Engineering applications of correlation and spectral analysis, p. 315. Wiley-Interscience, New York (1980)